

The Effect of Initial Velocity Model Accuracy on Refraction Tomography Velocity Model in Sefid-Zakhor Gas Field, Iran

Maryam Noori¹, Seyed Reza Shadizadeh^{2*}, Mohammad Ali Riahi³, Javad Jamali⁴

¹ M.Sc. Student of Exploration Petroleum Engineer, Abadan Petroleum University of Technology (PUT), Iran

² PHD, Petroleum University of Technology (PUT), Iran

³ PHD, Geophysics Institute of Tehran University, Iran

⁴ Geophysics Expert of Exploration Direction, Iran

Maryam.Exploration@yahoo.com or Maryam.Noori@put.ac.ir

Abstract: One of the limitations of velocity models obtained from seismic method is lack of lateral resolution at low frequencies, since in this method the stacking velocity is used. The major objective of this paper is to cover lateral resolution using refraction tomography. In refraction tomography modeling a correct initial velocity model based on refraction wave data is the main step for tomography inversion. The presented paper focuses on preparation of the initial velocity model for refraction tomography. This model is then used in seismic tomography process to minimize the time difference between the initial model and all first breaks. 31 km 2D wide-line seismic data of Sefid-Zakhor gas field are selected so that contain exploration well of the field to compare tomography inversion interval velocity model in well location with checkshot interval velocity for validation. The high fit between checkshot and tomography velocity is observed. High accuracy result is derived because of picking first time arrivals both in shotgathers and satationgathers and considers any lateral change as a velocity layer in preparing initial velocity model. However, in the Sefid-Zakhor gas field the data acquisition is discontinues because of its erratic terrain topography, the desired result obtained in the first iteration of refraction tomography inversion because of the accuracy of the initial velocity model. Finally, the drift between well and tomography velocity is applied to the area using MATLAB Software Packages.

[Noori M, Shadizadeh SR, Riahi MA, Jamali J. **The Effect of Initial Velocity Model Accuracy on Refraction Tomography Velocity Model in Sefid-Zakhor Gas Field, Iran.** *J Am Sci* 2012;8(9):505-514]. (ISSN: 1545-1003). <http://www.jofamericanscience.org>. 71

Keywords: Initial velocity model; Lateral velocity change; Refraction Tomography; SIRT; Misfit time

1. Introduction

An accurate seismic velocity modelling near the surface is the first and the most important step for processing and interpretation of seismic sections. Modifying the final velocity model for geophysics and interpreters is very important, because velocity is an important parameter in determining lithology, depth migration, reservoir characterization and even variation of fluid in oil reservoir. Correct distribution of velocity in the area for depth interpretations such as fault is more accurate and easier. Final velocity model updating can be achieved by near surface velocity model using seismic refraction processing. Usually first arrivals are direct wave or refracted rays. If the noise of area is low determination of first layers velocities from time-velocity curve are more reliable and correct than velocity determination from other seismic waves. Integrating the information from several kinds of waves, first-arrival tomography has the ability to estimate the velocity at each observation location and to build the near-surface velocity model (Li et al. 2000).

An accurate near surface velocity model could be used for geophysics' study of agricultural engineering to determine the depth of bed rock and soil depth. Also it would be useful in construction for dam structure, bed rock determination and underground water level. Archaeological structures can also be found by this technic.

In recent decades, near surface velocity model with very high accuracy has been achieved in the range of 100-200 m long and 400m depth using 3D and 2D refraction tomography. In this paper the range of 31km long and 1500 m depth of 2D seismic survey has been studied for near surface velocity model.

Refraction tomography has the ability to show lateral velocity changes. Therefore, the pore pressure can be computed, since pore pressure cause lateral velocity variations.

Refraction tomography has been used since the 70s. SIPT2 iterative ray tracing technique first introduced by Scott in 1973, in this technique a misfit between real and predicted data was computed. This misfit was very large for first iterative, so he repeat the iteration to conjugate the best fit. White (1989)

provides an overview. They mainly consist of a ray propagation computation and inverse projections such as iterative reconstruction techniques. Zhang and Toksoz (1998) address different inversion methods and resolution analysis. They implemented non-linear first-arrival tomography with regularization techniques. Practical details are covered by Lanz et al. (1998). Zhu et al. (1992) introduced bend rays into the tomographic inversion to determine near-surface velocity models. Stefani (1995) for Turning-ray tomography mentioned the phenomena of bend ray tomography. Li et al in 2000 fulfilled a first-arrival tomographic inversion by using rectangular grids to factorize the model and using a least-squares orthogonal resolution algorithm to iteratively solve tomographic equations.

If simple mathematical language used to describe the methods, all procedures are often referred to as ray tracing in a forward and reverse problem. The total travel time is the integral over the whole path l :

$$t = \int_0^L dt = \int_0^L \frac{dl}{v} = \int_0^L s dl \quad (1).$$

In M model cells of constant slowness s_i and transfer the integral into a sum:

$$t = \sum_{i=1}^M l_i s_i \quad \text{or} \quad T = LS \quad (2).$$

In ray tracing both Snell law and Hugen principle are used for refraction arrivals and the equation would be more complex considering the incidence angle and other parameters. Travel time T can be wrote as multiplication of matrix L and vector S .

Then an inverse problem used to find velocity distribution that is able to explain the measured travel times, i.e. to find an inverse operator.

$$s_{k+1} = s_k + \Delta s_k + L^{-1}(s_k)(t - L(s_k)s_k) \quad (3).$$

Then L is recomputed and so on. L^{-1} is used as inverse operator.

The first-arrival tomographic techniques have advanced a great deal in recent decades because many authors have been devoted overcoming the technical problems in this domain. Kutrubes et al in 1996 used nonlinear refraction travel time tomography technique of Zhang et.al (1996) to determine bedrock depth of coastal site in eastern Massachusetts, and locate areas where overburden thickness is sufficient for the construction of a replacement storm drainage system. An overview on refraction tomography as a practical emerging technology was done in 2001 by Konstantin Osypov. In this overview delay time method for refraction static was discussed. Generalized reciprocal method has been widely applied to 2-D data. Unfortunately, for 3-D seismic, it is difficult to apply due to the lack

of reciprocal data. However, the concept of delay times is useful for 3-D refraction statics calculations by assuming first arrivals to be the onset of head waves propagating along the refracting interfaces of locally flat layers on the scale of the offset range. Head-wave methods are in general robust because the relationship between the delay times and the observed travel times is linear (Osypov, 2001).

In order to map the archaeological structures (such as walls and burrows), Electrical resistivity tomography (ERT) and seismic-refraction tomography methods are used. Seismic velocity variations provide information about the geometrical features of the remains (G. Leucci et al 2006). Osazuwa and Chinedu in 2007 used refraction tomography process to provide a frame work for the characterization and mapping of subsurface channels for water seepage in the vicinity of dams. They found high velocity regimes whose values are comparable with those of the unweathered basement due to consolidated laterite, and low velocity zones indicating high permeable channels in form of loose ground within the overburden. In 2008 Chen Baofu et al used wide-line in the Tu-Ha area, West China, to identify thick near-surface structures by refraction tomography. Using this method they identify the depth of low velocity layer (LVL). Taillandier et.al, (2008) rectify Classical 3-D refraction travel time tomography algorithms because of their computational limitations due to the large datasets. They suggest a 3-D refraction tomography algorithm based on adjoint state techniques to derive the gradient of the travel time misfit function. Using synthetic and field data to investigate the effectiveness of commercial refraction tomography codes on both simple and complex subsurface velocity structures indicate that refraction tomography is able to resolve karst features under some conditions. (Jacob R. Sheehan, et al 2005). Armstrong F. Sompotan et al (2011) used refraction tomography for investigating shallow landslides In Indonesia.

2. Research Framework

The main aim of the present study is to create an initial velocity for refraction tomography. Then process the tomography on created initial velocity with the best refraction parameter and match tomography result with checks hot velocity to validate refraction tomography. This study is for depth deeper than surface structures.

3. Methodology

3.1 Geophysical Survey

The geophysical survey at the area is executed in 2003 over a 31km 2D explosive seismic survey (Fig. 1b). This survey includes 536 sources

and 1030 receivers with group interval 30m. The area has erratic terrain topography (Fig.1c).

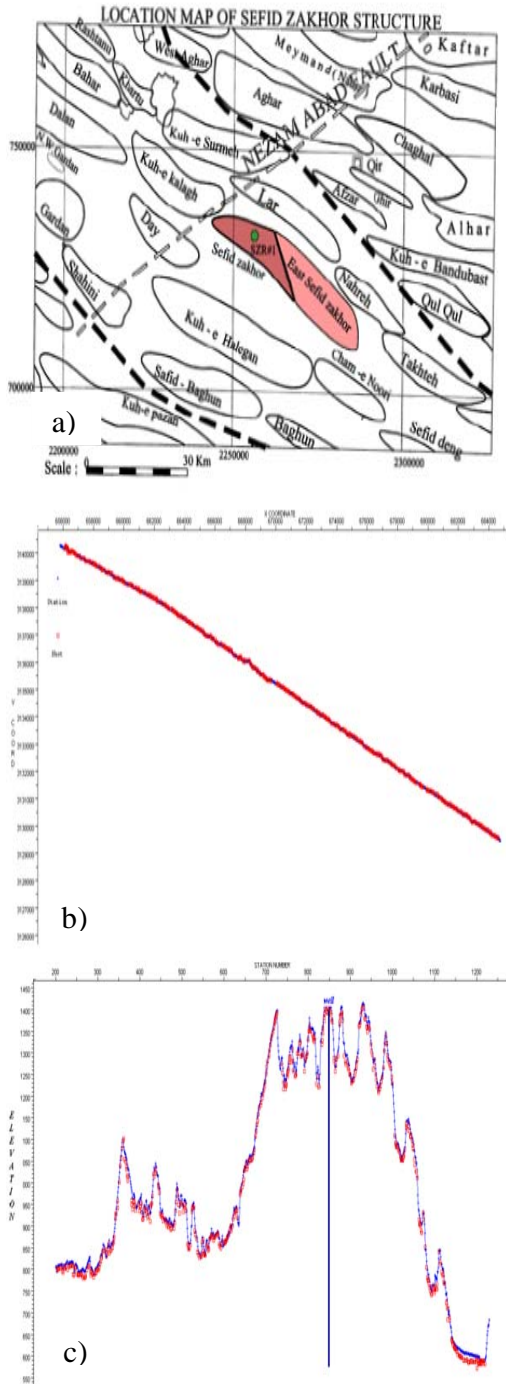


Figure 1. a). Sefid-Zakhor Geographical location. b). 2D seismic survey of the area. The red stars squares are shot point and the blue stars are the stations. c): surface topography.

3.2 Procedure

The research main three steps are:

- (1) Create high accuracy initial velocity model
- (2) Refraction tomography process by using ray tracing method of Um and Thurber (1987).
- (3) Matching the tomography results by well's check shot velocities

3.2.1 Create High accuracy initial velocity model

To create initial velocity model six steps are used (chart. 1).

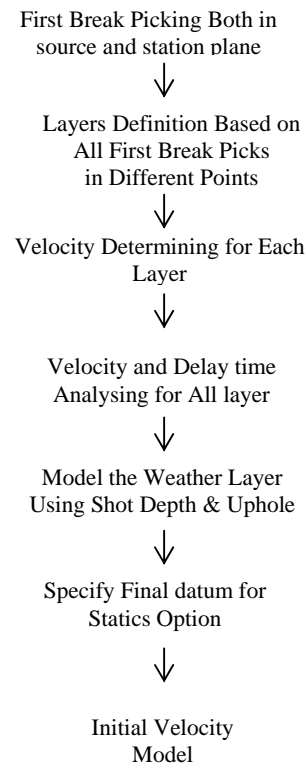


Chart 1. Initial Model Procedure

3.2.1.1 First Break Picking Both in Source Plane and Station Plane

First arrival time for observed time in ray tracing is picked here. To have accuracy first arrivals picked both in source plane and detector plane. First the first breaks picked in shotgathers in shot plane. The shot-step increment was 2, means that decussate. To have high accuracy and validation of shot plane, the detector plane also is checked, and the first arrivals are picked there, again (Fig. 2).

3.2.1.2 Layers Definition Based on All First Break Picks in Different Points

The whole area is swept to pick all first breaks, and then coverage is done to cover shotgather groups in order to find firstarrival trends as layers. To increase accuracy any small change was

considered as a velocity layer. This can ensure that lateral velocity changes will be modelled. 7 layers were detected (Fig. 3b). By 12 points whole area was swept, each point is a groups of first breaks (Fig. 3a).

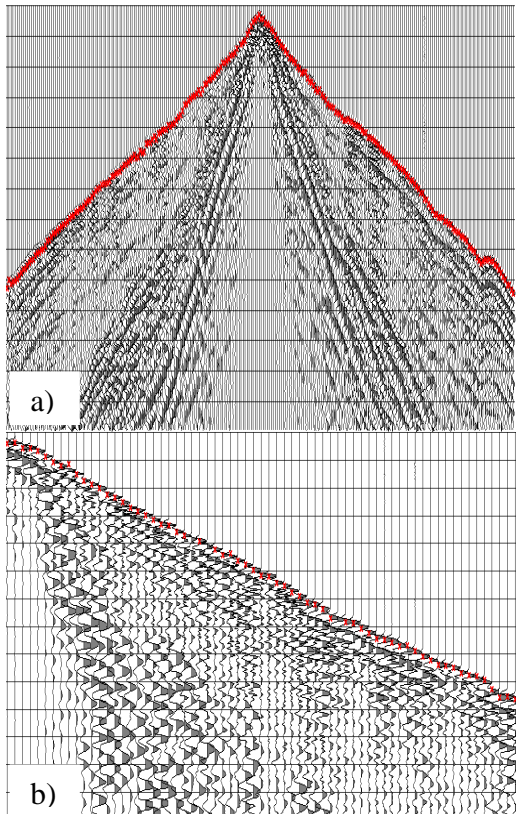


Figure 2. First break picking a) shot plane b) Receiver plane

3.2.1.3 Velocity Determining for Each Layer

For each layer from its slope the variation of velocity during the 12 points is calculated (Table. 1).

$$V_i = -(\text{slope of layer trend}) \quad (4)$$

Then out layers picks with maximum time error 80ms are rejected.

Table 1. Velocity Range of Each layer for velocity analysing

Layer#	Minimum Velocity(m/s)	Maximum Velocity(m/s)
Layer 1	1400	2900
Layer 2	2000	3900
Layer 3	3150	4100
Layer 4	3650	4750
Layer 5	3900	5100
Layer 6	4300	5500
Layer 7	4500	6700

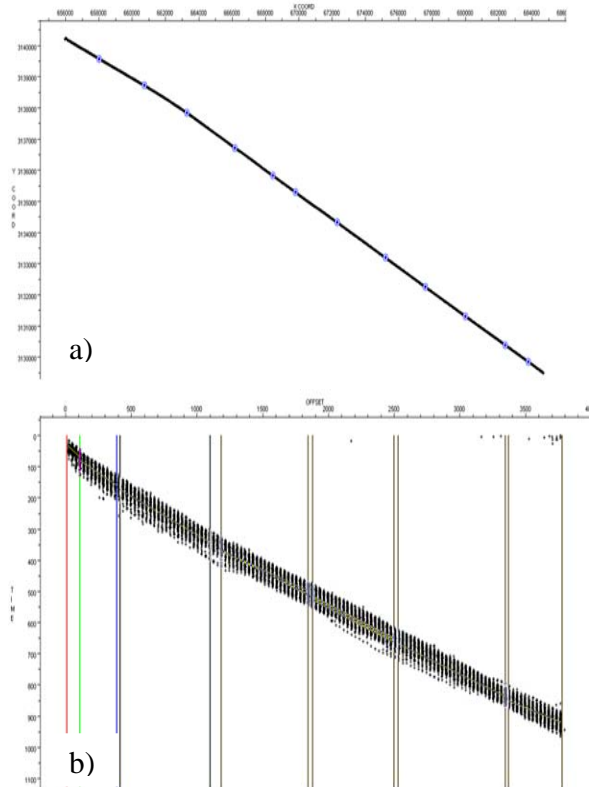


Figure 3. a) 12 point to sweep all picked shotgathers, each point is a groups of first breaks. b) offset vs time of a point. . 7 layers were detected to consider every lateral velocity changes.

3.2.1.4 Velocity and Delay Time Analysing for All Layers

The velocities of part 3 are analysed using reciprocal velocity analysing. The velocities of all refractors with 3shot-step is analysed and smoothed (Fig. 4). Then first delay time analysing is done using hybrid method. The Hybrid solution, as implied by the name, combines two algorithms, EGRM and Gauss-Seidel. Since the Hybrid technique creates a unique solution by uniting the long period solution of the EGRM with the short-period resolution of the Gauss-Seidel, it is also only appropriate for 2D data. Because the velocities are modified and are smoothed again a velocity analysing was done. The second delay time is done on data using The Extended Generalized Reciprocal Method (EGRM) method. The EGRM algorithm is appropriate for 2D data only. It requires a pre-existing velocity field. Delay times are calculated by examining reciprocal ray paths from pairs of shots into a common detector. The velocity field is used in calculating a compensation factor for offset shots and crooked survey geometries (Fig. 5).

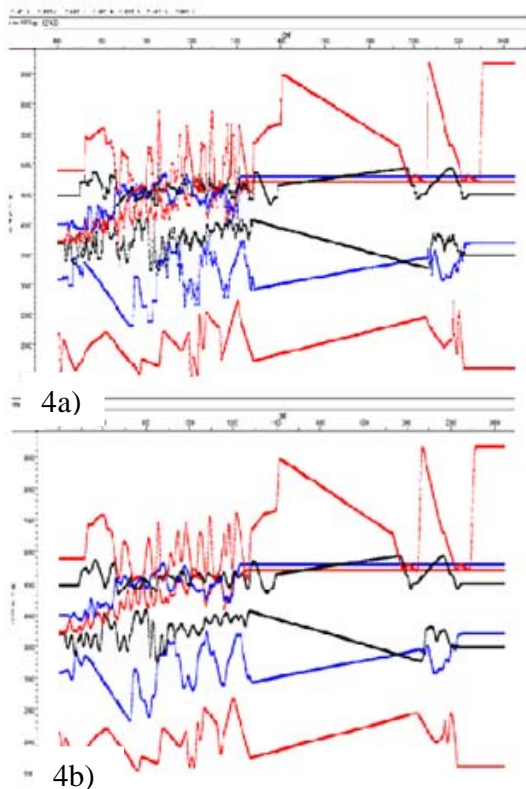


Figure 4. a) Analysed velocities for initial velocity model. b) Smoothed analysed velocity to reduce perturbations.

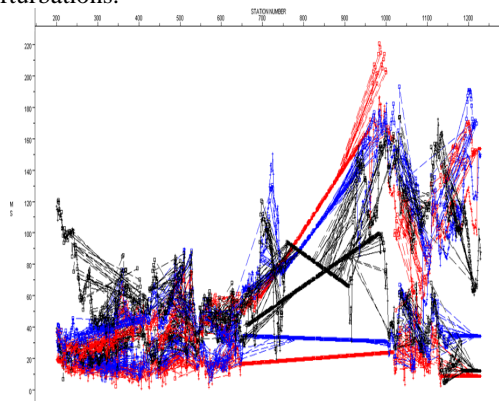


Figure 5. Delay times are calculated by examining reciprocal ray paths from pairs of shots into a common detector for all 7 layers.

3.2.1.5 Model the Weather Layer Using Shot Depth & Uphole Time

Since the shots were located in holes, the seismic data weren't from the surface elevation. So the weather layer (LVL) should be added as a layer to former 7 layers.

3.2.1.6 Specify Final datum for Statics Option

For static option final datum are needed. Final datum is defined with constant velocity of 3000 m/s at 1452 meter above sea level, about 10 meters above the highest surface elevation (Fig. 6).

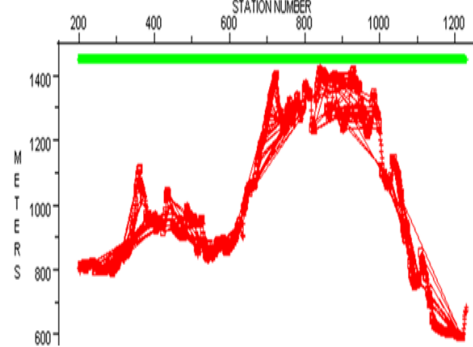
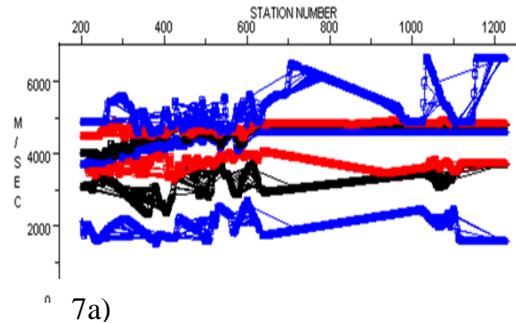


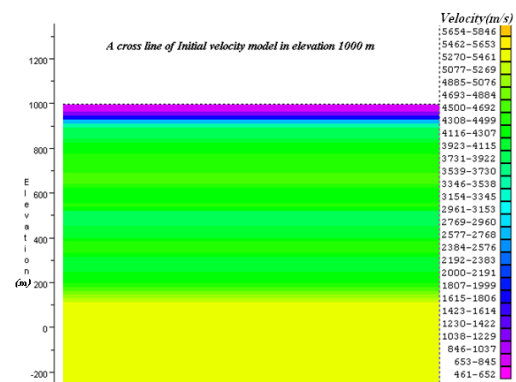
Figure 6. Final datum for static option. Final datum is defined with constant velocity of 3000 m/s at 1452 meter above sea level, about 10 meters above the highest surface elevation.

3.2.1.7 Initial Velocity Model

By combining these layers the initial velocity model is created (Fig. 7). For each layer based on x and y coordinate velocity, and elevation were out putted. These data were combined to make an ASCII file of initial velocity model.



7a)



7b)

Figure 7. a) Completed initial velocity model after velocity and delay time analysing on velocity layers. b) Initial velocity model cross line at elevation 1000.

3.2.2 Refraction Tomography Processing
Chart diagram of refraction tomography.

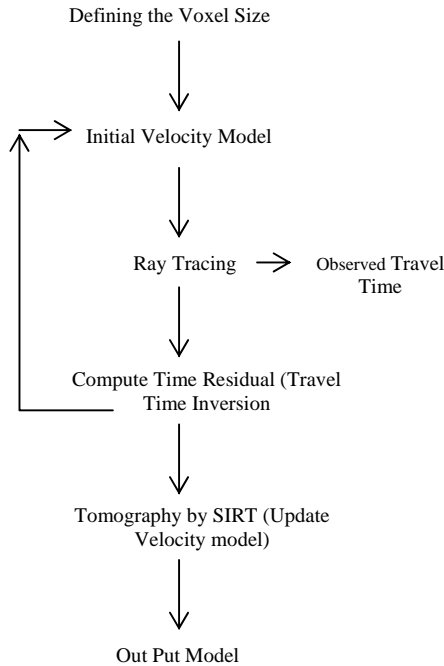


Chart 2. Travel time Tomography Workflow.

3.2.2.1 Defining the Voxel Size

Define the voxel size to cover the initial velocity model. The velocity model is represented by quadrangle cell. The width of an each cell is chosen as the receiver interval (G.Lucci, 2007). Voxel size needs to be large enough to contain a sufficient number of ray segments for solution reliability. The number of voxels in the image plane is the number of unknowns in the inverse problem. The number of source-receiver pairs determines the number of known parameters (travel times). This procedure has to be completed prior to the ray tracing.

The spread length in seismic data acquisition is usually longer than that in shallow refraction surveys, (Chen Baofu et al.; 2008). The depth of refraction ray penetration is about $\frac{1}{3} - \frac{1}{4}$ of seismic line. Since the depth of ray penetration is small compared to the length of a seismic line, it is usually advantageous to make the vertical voxel size smaller than the inline and crossline voxel sizes. As a general statement, the voxel size needs to be small enough to resolve the smallest feature of interest. At the same

time, voxel size needs to be large enough to contain a sufficient number of ray segments for solution reliability.

In this study 3 different voxel sizes, 30×20 , 30×12 and 28×17 are considered and the results are matched with checkshot velocity data. The minimum elevation for this study is -2000m.

3.2.2.2 Initial velocity Model

The modeled initial velocity as ASCII file is added to be covered by defined voxel (Fig. 8).

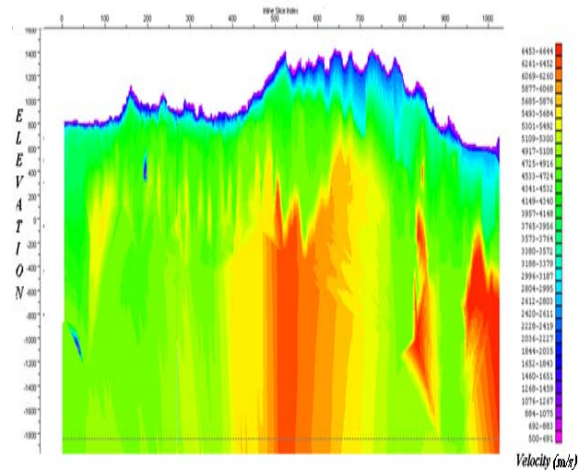


Figure 8. Final completed initial velocity model for velocity updating in refraction tomography covered by mesh grids 28×17 (m).

3.2.2.3 Ray Tracing tomography, Travel Time Inversion (SIRT)

Ray tracing and segmentation involve computing travel times and ray paths between a source and receiver pair and obtaining a ray segment in each voxel crossed by a ray path (Fig. 9). The segment lengths are used for calculating weights and updating the velocities during the inverse problem.

Each voxel is assigned a velocity value at its centre and any intermediate velocity values required for the ray tracer are interpolated to allow for inhomogeneity.

Segmentation:

$$t_m = \sum_{i=1}^I \sum_{j=1}^J \sum_{k=1}^K [S_{ijk}^q] D_{ijk} \quad (5)$$

Where:

t_m = computed travel time for the mth ray.

S_{ijk}^q = slowness in cell ijk at iteration q .

D_{ijk} = distance in cell ijk .

Above method is 3-D version of the Maximum Velocity Gradient ray tracing method of Um and

Thurber (1987). This method uses Fermat’s principle for ray tracing. The model is updated by the SIRT method for 5 iterations.

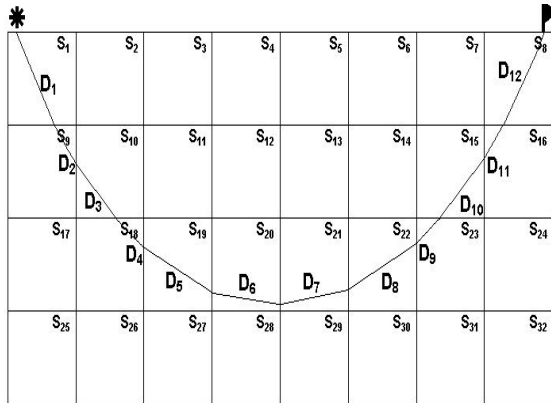


Figure 9. Travel time computation. Ray paths between a source and receiver pair in SIRT (Simultaneous Iterative Reconstruction Technique) ray tracing method (Um and Thurber; 1987).

3.2.3 Well and Tomography Velocity Matching

To obtain tomography velocity result in well location a harmonic average is done based on the distance of the 4 cells from well location. The well was located on the middle of these four cells (Fig. 10).

$$V_{av} = \frac{\sum_{i=1}^4 \left(\frac{1}{d_i} * V_i \right)}{\sum_{i=1}^4 \left(\frac{1}{d_i} \right)} \quad (6)$$

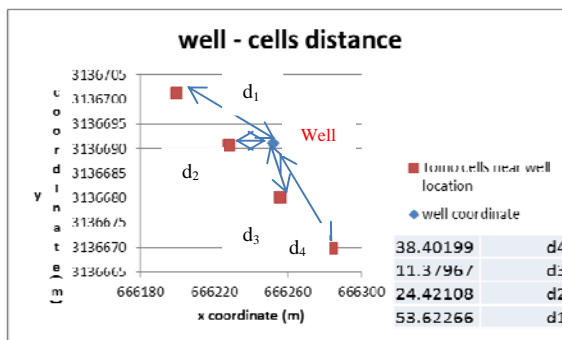


Figure 10. Well location between four cells of tomography voxels. Harmonic average used to obtain tomography interval velocity in the well location using these cells velocities.

4. Results

The first objective of the study is to develop an accurate initial velocity model of the area. To

consider small velocity changes both in vertically and laterally, seven refractors are detected. After velocity and delay time analysing on these velocity layer the initial velocity model is completed (Fig. 7). Then weathered layer from shot depth and uphole time is added to the mode. Also final datum for static option is calculated (Fig. 6). Figure 8 showed the final completed initial velocity model.

Tomography refraction for 5 iterations is done on initial velocity model for 3 different voxel sizes, 30 × 12, 30 × 20, and 28 × 17. The group interval of receivers in this study was 30m (Fig. 11). Usually a quadrangle voxel sizes with the receiver’s distances are considered. But since the depth of refraction ray is less than seismic line, for vertical dimension $\frac{1}{3}, \frac{1}{2}, \frac{1}{2}$ of receiver’s distance is used separately. Figure 12 shows the match of tomography velocity in well coordinate of these scenarios with check shot velocity. Finally the result shows that in this area voxel size 28×17, a half-length of receiver interval for vertical size, Give the best result and has an excellent match with check shot velocity (Fig. 12c). The well was located between the cells coordinates, and there were no cell with exact well coordinate. The nearest four cells to well location are detected and a harmonic average is done based on distance from well coordinate. Figure 10 shows these points and well location. The average result can be observed in table 2.

Table 2. a) Checkshot interval velocity of the well

rec_elev(m)	TVD(m)	Vint(m/s)
1061	304.3	4150.0361
816	548.8	4467.8811
583	781.3	5751.5708
464	900	5500
456	908	5172.4138
162	1201.3	3778.3375
0	1363.1	4355.7169
-24	1387	4761.9048
-91	1454	5282.5553
-349	1711.8	5274.7253
-397	1759.8	5683.8472
-1352	2714.4	5663.2653

Table 2. b) Harmonic average on tomography results of the nearest four cells to well location

Depth (m)	Harmonic average of interval velocity (m/s)	Depth (m)	Harmonic average of interval velocity (m/s)

	(Tomo) for well location		(Tomo) for well location
1260.9	4571.174	512.9	5135.616
1243.9	3392.678	495.9	4900.173
1226.9	2558.254	478.9	4727
1209.9	2230.615	461.9	4645.835
1192.9	2325.835	444.9	4618.106
1175.9	2457.279	427.9	4607
1158.9	2568.338	410.9	4576.106
1141.9	2677	393.9	4508
1124.9	2790.721	376.9	4306.059
1107.9	2922.384	359.9	4175.721
1090.9	3097.443	342.9	4317.557
1073.9	3275.164	325.9	4560.059
1056.9	3411.886	308.9	4681
1039.9	3562.548	291.9	4693
1022.9	3766.886	274.9	4688.338
1005.9	3968.886	257.9	4662.835
988.9	4120.886	240.9	4548.165
971.9	4227.548	223.9	4377.827
954.9	4302.548	206.9	4254.721
937.9	4382.721	189.9	4193.721
920.9	4492.105	172.9	4138.721
903.9	4613.721	155.9	4081.827
886.9	4731	138.9	3987.059
869.9	4812.835	121.9	3903.662
852.9	4857.338	104.9	3858
835.9	4879.338	87.9	3852
818.9	4910.279	70.9	3857
801.9	5027.836	53.9	3876
784.9	5150.114	36.9	3926
767.9	5222.452	19.9	4021
750.9	5241.22	2.9	4213
733.9	5260.114	-14.1	4656
716.9	5265.114	-31.1	4967
699.9	5286.114	-48.1	5137
682.9	5314.114	-65.1	5137
665.9	5340.009	-82.1	5137
648.9	5337.173	-99.1	5137
631.9	5374.73	-116.1	5137
614.9	5451.895	-133.1	5137
597.9	5541.557	-150.1	5137
580.9	5596.722	-167.1	5137
563.9	5562.451	-184.1	5137
546.9	5469.663	-201.1	5137
529.9	5329.663	-218.1	5137

5. Discussions and Conclusions

In this research a high match between well and tomography velocity is generated. Since for initial velocity model we make effort to consider any change in time offset curve as a velocity layer. So almost all lateral velocity changes in the area are modelled. However, usually geophysics interpreters

consider three layers for initial velocity model in velocity updating.

Figure 12c shows a small drift between check shot and tomography velocity. To remove this drift a relationship between check shot and tomography velocity is obtained. A cross plot (Fig.13), between well and tomography result generated; the following relationship. Small tomography drift is corrected using a matlab code on whole area and the corrected velocities saved as Ascii file. This Ascii file is mapped. Figure 14 shows these maps, the final tomography velocity model before and after correction.

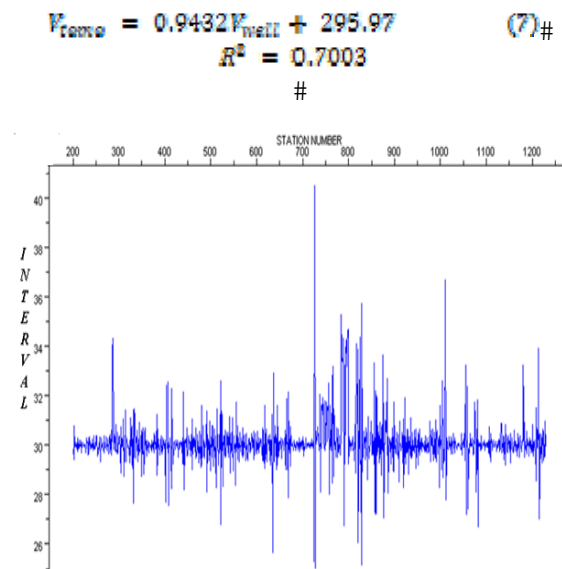


Figure 11. Group interval of stations, almost all station has group Interval of 30, so it is the best width for horizontal mesh grid size.

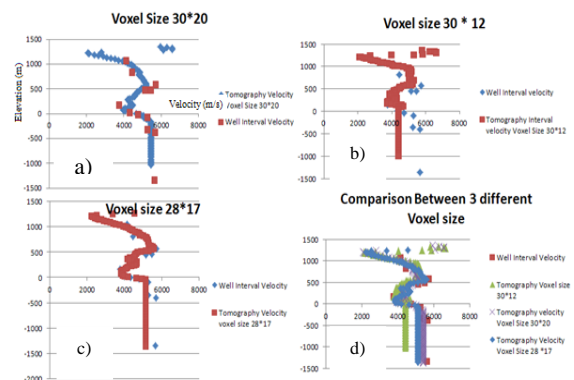


Figure 12. Match of tomography velocity in well coordinate of three different voxel sizes with check

shot velocity. Voxel size 28×17, a half-length of receiver interval for vertical size, Give the best result and has an excellent match with check shot velocity.

The second note in this study is that in the first iteration the best results are generated, and with increasing the number of iteration the misfit between well and tomography is increased (Fig. 15). It's may be because of perturbation of ray tracing. Since the minimum elevation was considered to be -2000m. The ray penetration of refraction wave may be less or higher than this elevation. However zero depth for minimum elevation for 28×17 voxel size is tested. But again the misfit increase for higher iterations. By the way, because of high accuracy of initial velocity model the best fitting is generated at the first iteration.

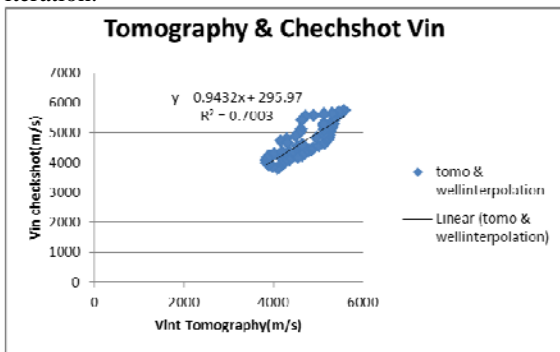


Figure 13. Relationship between interval velocity of tomography and check shot.

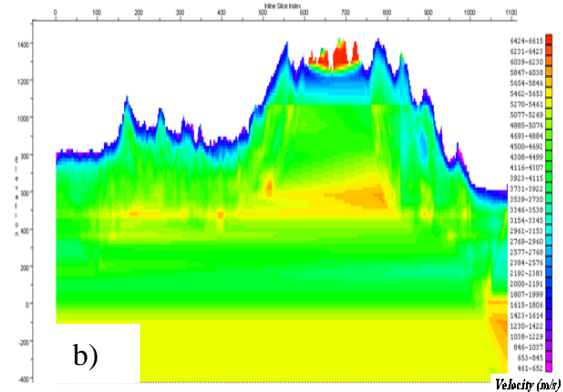
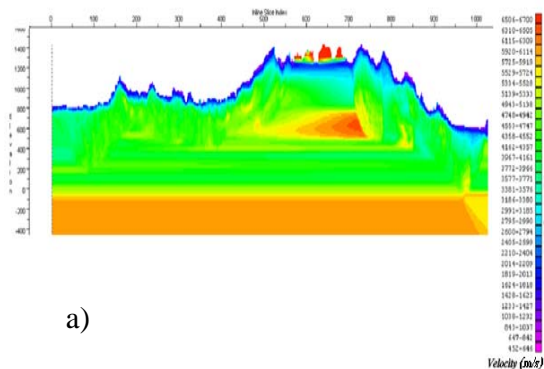
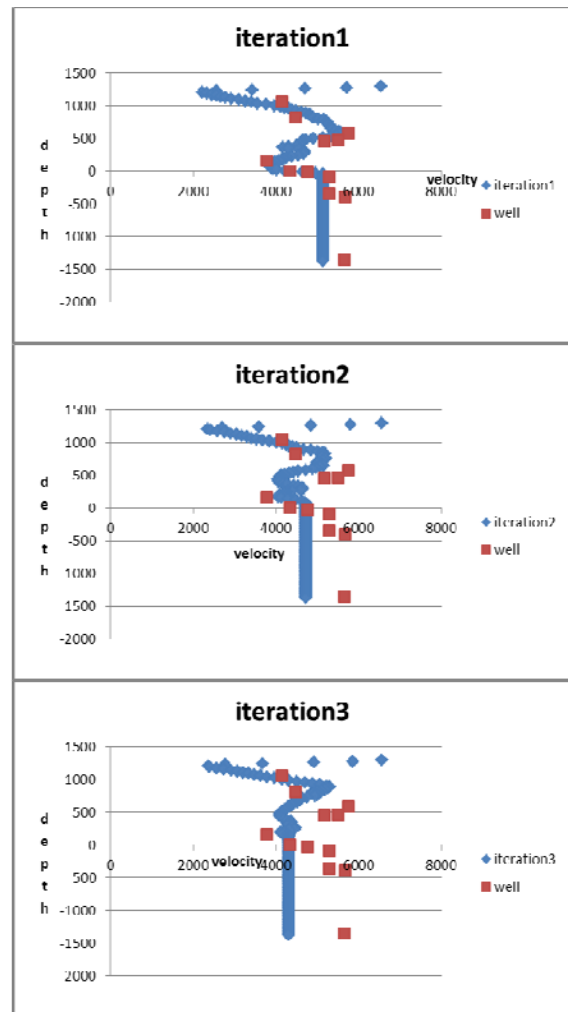


Figure 14. . Final tomography velocity model before and after correction. a) Befor drift correction. b) After drift correction



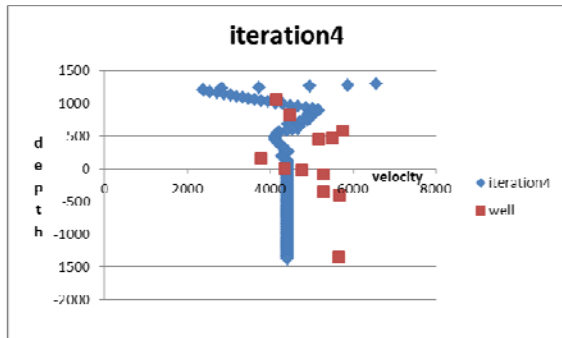


Figure 15. By increasing the number of iteration the misfit between well and tomography is increased because of perturbations. The best result was generated in the first iteration.

Acknowledgment

Our profound gratitude goes to NIOC Exploration Direction (Exploration Direction of National Iranian OIL Company) for making available, the equipment, soft wares, and financial support for this research.

Corresponding Author:

Dr. Seyed Reza Shadizadeh
 Department of petroleum Engineering
 Abadan Faculty of Petroleum Engineering
 Petroleum University of Technology
 Northern Bowarde,
 Abadan, Iran, 6318714331.
shadizadeh@put.ac.ir

References

1. Scott, J. Seismic refraction modeling by computer: *Geophysics*, 1973;38(2): 271-284.
2. Um, J., and C. H. Thurber. A fast algorithm for two-point seismic ray tracing, *Bull. Seism. Soc. Am.* 1987;77: 972–986.
3. White, D. J. Two-dimensional seismic refraction tomography. *Geoph. J. Int.*1989;97: 223–245.
4. Zhang, J., and Toksoz, M. N. Nonlinear refraction travelttime tomography, *Geophysics* 1998; 63(5): 1726-1737.
5. Lanz, E., Maurer, H., and Green, A. G. Refraction tomography over a buried waste disposal site. *Geophysics* 1998; 63(4): 1414–1433.
6. Zhu et al. Recent applications of turning-ray tomography, *Geophysics* 2008; 73(5): 243-254.
7. Zhu, X., Sixta, D. P., and Angstman, B. G. Tomostatics: Turningray tomography + static correction: *The Leading Edge* 1992; 11: 15-23
8. Stefani, J. P. Turning-ray tomography: *Geophysics* 1995; 60:1917–1929.
9. Kutrubes, D.L., Zhang, J., and Hager, J. (proof-reader). Conventional processing techniques and nonlinear refraction travelttime tomography for imaging bedrock at an eastern Massachusetts coastal site, *Symposium for the Applications of Geophysics to Environmental and Engineering Problems*, April 1996, Keystone, CO.: 215-220
10. Li, L., S. Luo, and B. Zhao. Tomographic inversion of first break in surface model: *Oil Geophysical Prospecting* 2000; 35: 559–564
11. Konstantin Osypov. Refraction tomography: a practical overvoiew of emerging technologies, *CSEG Recorder WesternGeco*, Denver, Colorado, USA 2001; :5-8
12. G. Leucci , F. Greco, L. De Giorgi , R. Mauceri. Three-dimensional image of seismic refraction tomography and electrical resistivity tomography survey in the castle of Occhiola` (Sicily, Italy), *Journal of Archaeological Science* 2007; 34: 233-242
13. I.B. Osazuwa, A.D. Chinedu. Seismic refraction tomography imaging of high permeability zones beneath an earthen dam, in Zaria area, Nigeria, *Journal of Applied Geophysics* 2008;66 : 44–58
14. Chen Baofu, Xiong Dingyu, Ren Xiaoqiao and Cheng Chunhua. The first-arrival tomographic inversion and its application to identify thick near-surface structures, *SEG Las Vegas* 2008; :3255-3259.
15. C. Taillandier, M. Noble , H. Calandra , H. Chauris, P. Podvin . 3-D Refraction Travelttime Tomography Algorithm Based on Adjoint State Techniques, 70th EAGE Conference & Exhibition — Rome, Leveraging Technology 2008;:163-168.
16. Jacob R. Sheehan, William E. Doll, David B. Watson, Wayne A. Mandell. Problems Detecting Cavities With Seismic Refraction Tomography: Can It B Done?, 18th EEGS Symposium on Application of Geo physics to Engineering and Environmental Session: Seismic Refraction Applications 2005. Armstrong F. Sompotan, Linus A. Pasasa, Rachmat Sule. Comparing Models GRM, Refraction Tomography and Neural Network to Analyze Shallow Landslide, *ITB J. Eng. Sci* 2011;43(3):161-172

7/26/2012